



**HAL**  
open science

## Synthesis and Characterization of Thermosetting Polymers: An Electrospinning Approach

Alexander Fainleib, Olga Grigoryeva, Olga Starostenko, Daniel Grande

► **To cite this version:**

Alexander Fainleib, Olga Grigoryeva, Olga Starostenko, Daniel Grande. Synthesis and Characterization of Thermosetting Polymers: An Electrospinning Approach. IntechOpen. Advances in Nanofiber Research - Properties and Uses, 7 (5), IntechOpen, pp.1-22, 2024, Nanotechnology and Nanomaterials, 978-1-83769-780-9. 10.5772/intechopen.1007735 . hal-04864164

**HAL Id: hal-04864164**

**<https://hal.science/hal-04864164v1>**

Submitted on 10 Jan 2025

**HAL** is a multi-disciplinary open access archive for the deposit and dissemination of scientific research documents, whether they are published or not. The documents may come from teaching and research institutions in France or abroad, or from public or private research centers.

L'archive ouverte pluridisciplinaire **HAL**, est destinée au dépôt et à la diffusion de documents scientifiques de niveau recherche, publiés ou non, émanant des établissements d'enseignement et de recherche français ou étrangers, des laboratoires publics ou privés.



Distributed under a Creative Commons Attribution 4.0 International License

# We are IntechOpen, the world's leading publisher of Open Access books Built by scientists, for scientists

7,200

Open access books available

192,000

International authors and editors

210M

Downloads

Our authors are among the

154

Countries delivered to

TOP 1%

most cited scientists

14%

Contributors from top 500 universities



WEB OF SCIENCE™

Selection of our books indexed in the Book Citation Index  
in Web of Science™ Core Collection (BKCI)

Interested in publishing with us?  
Contact [book.department@intechopen.com](mailto:book.department@intechopen.com)

Numbers displayed above are based on latest data collected.  
For more information visit [www.intechopen.com](http://www.intechopen.com)



Chapter

# Synthesis and Characterization of Thermosetting Polymers: An Electrospinning Approach

*Alexander Fainleib, Olga Grigoryeva, Olga Starostenko and Daniel Grande*

## Abstract

This chapter is devoted to the description of the main recent approaches and technical solutions for the creation of polymer micro- and nanofibers engineered by electrospinning precursors of thermosetting polymers. Structure-property relationships have been analyzed for miscellaneous complex systems, including epoxy electrospun micro and nanofibers; submicron carbon nanotube–epoxy nanocomposite filaments, rigid fibers based on functional polynorbornenes with epoxy or carboxylic pendant groups, and core-shell nanofibers with a structure of semi-interpenetrating polymer network (semi-IPN) based on thermoplastic polyamide and thermosetting epoxy resin. The first experimental results for creating electrospun nanofibers with a semi-IPN structure based on polysulfone/polycyanurate or polysulfone/polycyanurate/polybenzoxazine are discussed. Due to the unique properties of polycyanurates, namely high heat- and chemical resistance to aggressive substances, low dielectric losses, and low water absorption, the resulting electrospun fibers could potentially become useful as components in different advanced materials with improved properties to operate in aggressive environments over a range of temperatures.

**Keywords:** electrospinning, micro-/nanofibers, polysulfone, cyanate ester resins, thermosets

## 1. Introduction

Electrospinning has attracted significant attention as a manufacturing process for producing fiber materials with diameters ranging from the micro- to nanometer scales [1]. One such technique provides a promising and straightforward way to fabricate infinite and continuous fibers applied as nanostructured and biomedical materials [2, 3]. Electrospun nanofibers exhibit exceptional characteristics, including a high surface-to-volume ratio, permeability, absorbance capacity, porosity, interconnected ultrafine fibrous structure, and low weight. Electrospun fibers in nanoscale diameters have enticed wide consideration from researchers, who are ready to move toward a practice-based

interdisciplinary approach in a variety of fields [4–9]. A wide range of materials, such as engineered and biological polymers, ceramics, and composites, have been successfully electrospun into one-dimensional materials having many different microstructures [10]. Due to their remarkable characteristics, such as very small fiber diameters, large surface area per mass ratio, high porosity along with small pore sizes [3, 11], flexibility, and superior mechanical properties [12], nanofiber mats have found numerous applications in biomedicine (drug delivery, tissue engineering, and wound dressing), filtration, reinforcement in composite materials, protective clothing, and microelectronics (sensors, batteries, display devices, supercapacitors, and transistors) [13–18].

Most of the polymers are dissolved in a solvent before electrospinning, as the processing conditions involved are simple and straightforward. Moreover, polymers that melt at high temperatures can be fabricated into nanofibers through electrospinning; nevertheless, much fewer polymers have been electrospun from such a state [9, 19]. Importantly, all the polymers used for electrospinning were thermoplastics, which means soluble and meltable. Electrospinning of thermally reactive oligomers that result in significant thermosets constitutes a real challenge. This contribution addresses the fabrication of micro- and nanofibers containing thermosetting polymers with a special focus on polysulfone/polycyanurate (PSF/PCN) fibrous materials.

## 2. Principles of electrospinning

Continuous nanofibers and fibers of desired dimensions can be produced by the electrospinning technique [18]. This process also offers the possibility to form various fiber assemblies, including nonwoven, aligned or patterned fiber meshes, haphazard 3D structures, and tangled fibers [19]. Both natural and synthetic polymers, liquid crystals, suspensions of solid particles, ceramics and emulsions can be used to produce ultrafine fibers with diameters ranging from 2 nm to 10  $\mu\text{m}$  by the electrospinning approach [20, 21].

**Figure 1a, b** shows a typical electrospinning setup that consists of a capillary tube with a needle, a high-voltage supplier, and a collecting screen [23]. Taylor [24] found that 6 kV applied voltage is required for the initiation of the electrospinning process to take place.

A syringe pump with a feeding rate of 0.1–60 mL/h is required for the electrospinning process [25] as well as a spinneret (clip spinneret, tube-less spinneret, coaxial spinneret, or heating spinneret) and collector (plate collector, rotary drum collector,

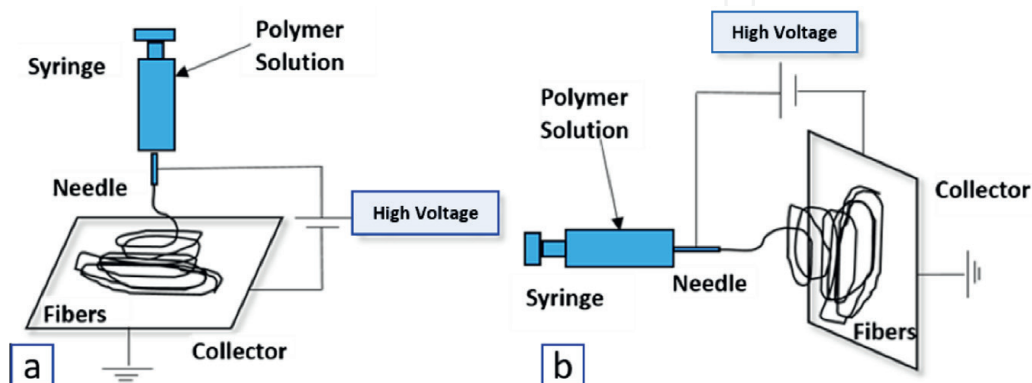


**Figure 1.** Schematic diagram of set-up of electrospinning apparatus (a) vertical set-up and (b) horizontal setup [22].

grid type collector, edge type collector, mandrel collector, steel sheet collector, or dual rings collector) [21]. Solution parameters (effect of dielectric property of solvent, surface charge density, surface tension, solution viscosity, polymer molar mass, and concentration), process parameters (effect of voltage, flow rate, collector type, and distance between needle tip and collector), type of spinning setup, and ambient parameters (effect of temperature and humidity) are responsible for the variations in morphology and diameters of the nanofibers produced by electrospinning [26]. Almost all soluble or fusible natural or synthetic polymers, as well as their blends, can be used for electrospinning [27]. This broad variety of polymers belongs to thermoplastics and comprises nucleic acids, proteins, and polysaccharides [28].

### 3. Nanofibers fabricated by electrospinning epoxy-based polymers

Recently, some publications have appeared on thermoset-containing nanofibers fabricated by electrospinning [29].

Epoxy is a thermosetting precursor that chemically reacts to form a crosslinked matrix when combined with a curing agent. Shneider et al. [29] demonstrated that to produce continuous micro- and nanofibers through electrospun epoxy, one must control the curing reaction with precision. For this purpose, epoxy and triamine curing agent were dissolved in a tetrahydrofuran–dimethylformamide (THF-DMF) binary solvent. The authors determined a narrow working window at which a proper solution for electrospinning is close to the gel point, right before the transition from liquid to solid gel state. The solution was characterized by means of (i) Fourier-transform infrared spectroscopy (FTIR) to control the curing process, (ii) steady shear viscosity to detect the divergence near the gel point, and (iii) oscillatory loss and storage shear moduli to identify the liquid-to-gel transition. The chemical transformations of epoxy solution, including chemical interconnections and gelation, could be monitored through these measurements, allowing for a working window to be defined for electrospinning.

Aliahmad et al. [30] described the electrospinning fabrication process (**Figure 2**) and characterization of submicron carbon nanotube (CNT) – epoxy nanocomposite

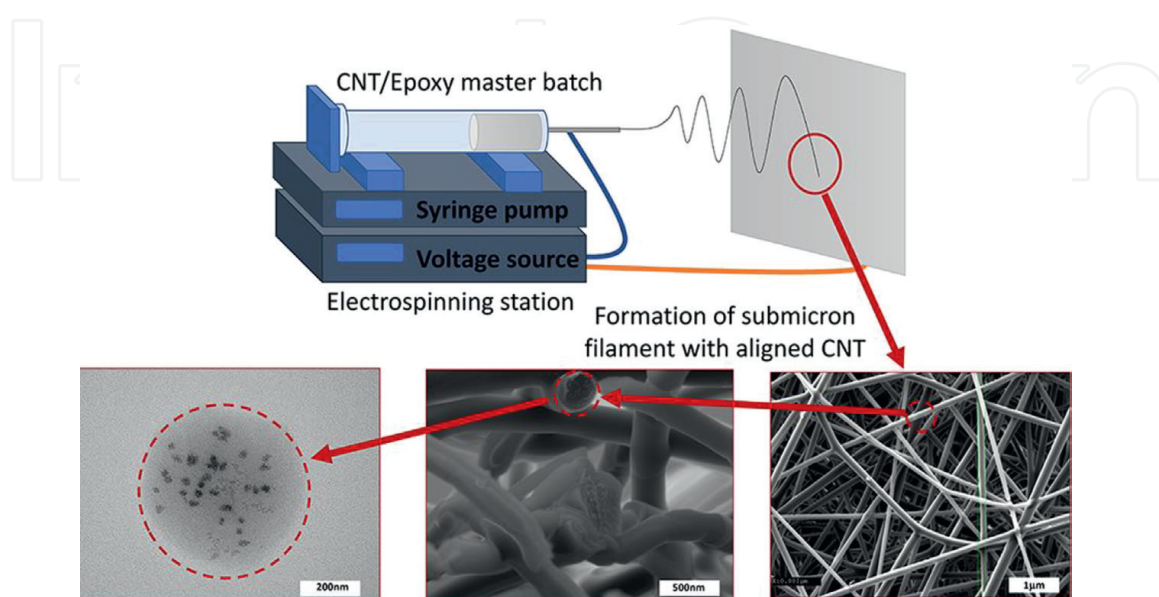


**Figure 2.** Schematic process for electrospinning a submicron CNT/epoxy filament [30].

filaments. Electrospinning of submicron epoxy filaments was carried out by partial thermal curing of the epoxy resin with the hardener without any thermoplastic component. This semi-curing approach made the epoxy solution viscous enough for the electrospinning process. The electrospun filaments were fabricated using a CNT/epoxy solution in DMF with a viscosity of 65 cP using 16 kV and a collector distance of 10 cm. The diameter of these filaments could be tuned to as low as 100 nm with the adjustment of electrospinning parameters. Better structural, electrical, and thermal stabilities were achieved by incorporating a low amount of CNT into epoxy. As a result of the electrostatic field during the electrospinning process, the CNT fibers were aligned within the epoxy filaments. The improvement of modulus up to 49% for CNT/epoxy filaments compared to epoxy was found. The authors concluded that the developed filament was suitable for many applications due to the use of a commercial epoxy suitable for industrial composite productions.

Two functional polynorbornenes (PBNEs), one bearing an epoxy pendant group and another one bearing carboxylic pendant groups, were electrospun in the presence of a variety of cross-linkers [31], resulting in long (several mm), rigid fibers with diameters that can be tuned in the range of 300 nm–10  $\mu\text{m}$  and glass transition temperatures ( $T_g$ s) higher than 300°C. A 20 kV positive voltage was applied to the needle tip. Despite being brittle, these fibers formed a continuous nonwoven mat, which was similar to any textile mat. Remarkably, injection rates as high as 1 mL/min could be used to prepare the fibers. Commarieu et al. [31] explained such a surprising result by the low propensity of entanglement for solutions of rigid-rod polymers. Curing of the fibers was performed by leaving the fibers 2 hours at 200°C. Once cross-linked, the fibers did not swell and became insoluble. The electrospinning process was used to encapsulate dyes or graphitic dots (GDs) (**Figure 3**). Due to the high cross-linking density of the fiber, dye leaching was prevented. In contrast with other rigid-rod polymers, electrospinning of PNBE is facile and can be performed at injection rates

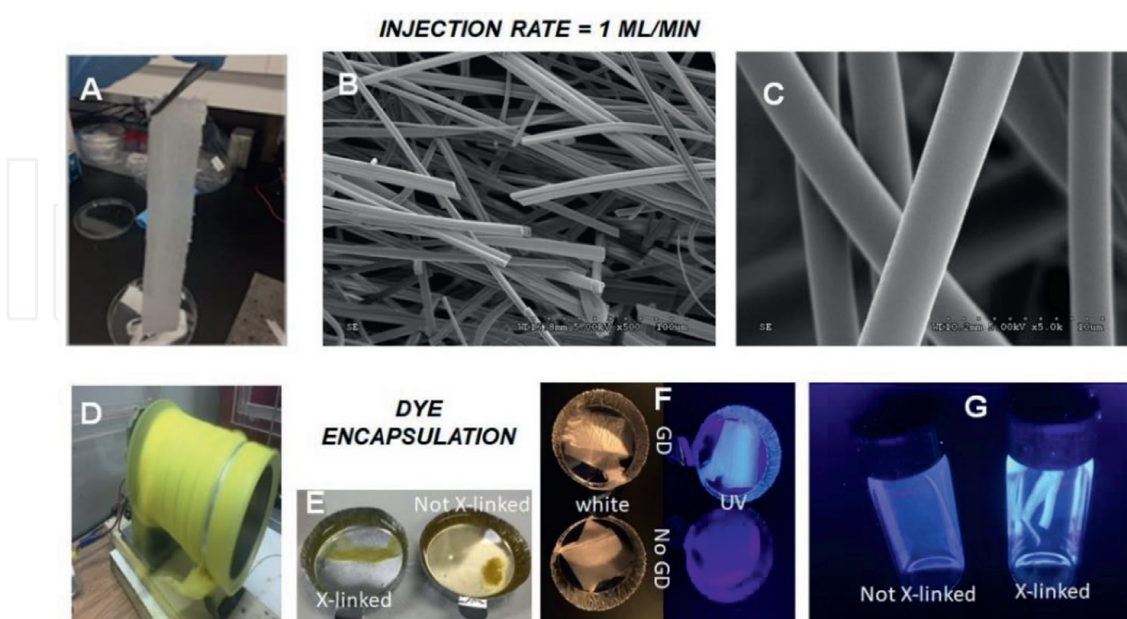


**Figure 3.** Mat of fibers obtained at high injection rate (1 mL/min) (a) and SEM pictures of the fibers (b, c). Cylindrical collector with fibers containing a yellow dye after 5 minutes of electrospinning (d) and same fibers immersed in THF, (e) before and after cross-linking. Pictures of fibers containing GDs under white and UV light (f) compared with fibers devoid of GDs. GD-containing fibers before and after cross-linking immersed in THF, under UV light (g) [31].

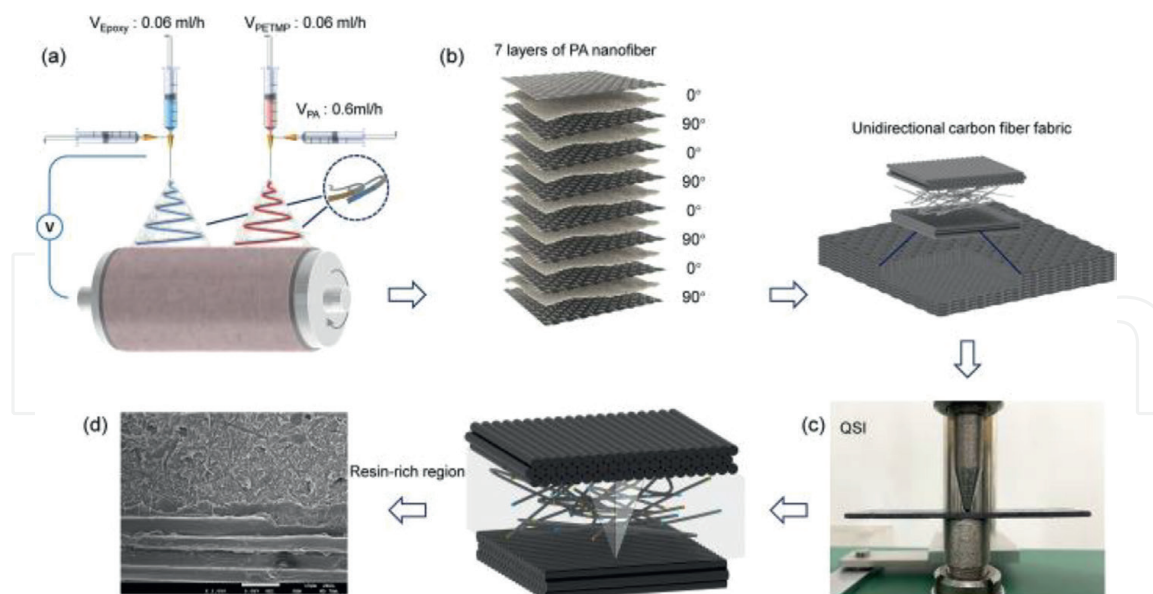


**Figure 4.** Schematic diagram of self-healing composites based on PA core-shell nanofiber: (a) preparation of PA core-shell nanofiber, (b) self-healing composites, (c) quasi-static indentation test, and (d) the PA core-shell nanofiber healed interlaminar damage [33].

as high as 1 mL/min. Due to their unique photophysical properties, GD-containing PNBE fibers could potentially become useful photocatalysts or fluorescent materials and as components in antibacterial textiles [32].

Core-shell nanofibers were prepared by coaxial electrospinning of a mixture of thermoplastic polyamide (PA) and thermosetting epoxy resin (ER) on the premise that the melting temperature of PA matches the curing temperature of the ER healing agent [33] (**Figure 4**). Such a combination without any chemical interactions between both polymeric components is called semi-interpenetrating polymer network (semi-IPN) [34]. The morphological and chemical study proved the core-shell structure of the nanofibers without any chemical reactions. The PA shell and the two-component epoxy core acted together as the healing agent to fill microcracks. Using this producing method allowed for obtaining self-healing composites possessing enhanced healing efficiency and responsiveness as well as the toughened interlaminar region (the bending strength of the composite having the embedded core-shell nanofiber was increased by 16%). Heating the composite samples at 130°C for 20 minutes after damage provided the healing effect for the composite containing neat PA nanofiber around at 62% and for the one with PA core-shell nanofiber at around 90%. The authors noted that the thermoplastic PA nanofiber had a good healing function and rapid healing responsiveness. It was found that the encapsulated thermosetting healing agent improved the healing efficiency of thermoplastic PA. Thus, electrospun core-shell nanofibers obtained from polymer combinations as semi-IPN-type are promising for healing agent encapsulation systems.

#### 4. Polysulfone-based electrospun thermoplastic nanofibers

Scientific specialists in the field of membranes pay special attention to polysulfone, namely a widely used thermoplastic polymer in microfiltration [35]. Polysulfone has a unique set of useful physical properties: high mechanical strength, destruction temperature (> 400°C), glass transition temperature (150–180°C), and resistance to aggressive

environments with different pH values. Polysulfone can be dissolved in aprotic polar solvents, such as dimethylsulfoxide, dimethylacetamide, dimethylformamide, nitrobenzene, and their halogen-containing derivatives [36–39], which is very important in the manufacture of membranes. As a rule, polysulfone membranes are obtained by the phase inversion method [40–43], the disadvantages of which are the limited range of pore sizes in the membrane and residual solvent, which affect the quality of the membranes [44].

The electrospinning technique is free from the abovementioned disadvantages and is effectively used to produce highly porous nonwoven mats with interconnected pores and a highly effective surface area suitable for large-scale production [45–48]. Membranes obtained by the traditional method are inferior to those produced by the electrospinning technique in flux performance at equal rejection efficiency [49]. The effect of the solution concentration (15, 20, and 25 wt.%) of polysulfone in dimethylformamide, voltage (12.5, 15, and 18 kV), and solution feed rate (1.5, 2.5, and 3.5 ml/h) on the morphology of the obtained fiber samples was systematically studied [35]. The SEM results showed that the samples obtained from a solution with a concentration of 15 wt.%, possessed a bead-on-a-string type morphology, and the homogeneous fiber samples without compactions and with an average diameter from 0.876 to 2.078  $\mu\text{m}$  depending on the voltage and feed rate were produced from solutions with a higher polysulfone concentration. The authors recorded the optimal combination of electrospinning parameters (solution concentration of 25 wt.%, feed rate of 3.5 ml/h and voltage of 18 kV) for obtaining high-quality fibers [35].

The THF-DMF binary solvent system with different ratios and dielectric constants ( $\epsilon$ ) from 16.33 to 27.97 was used for preparing smooth surface electrospun polysulfone nanofibers, while THF alone ( $\epsilon = 7.60$ ) and DMF alone ( $\epsilon = 36.70$ ) led

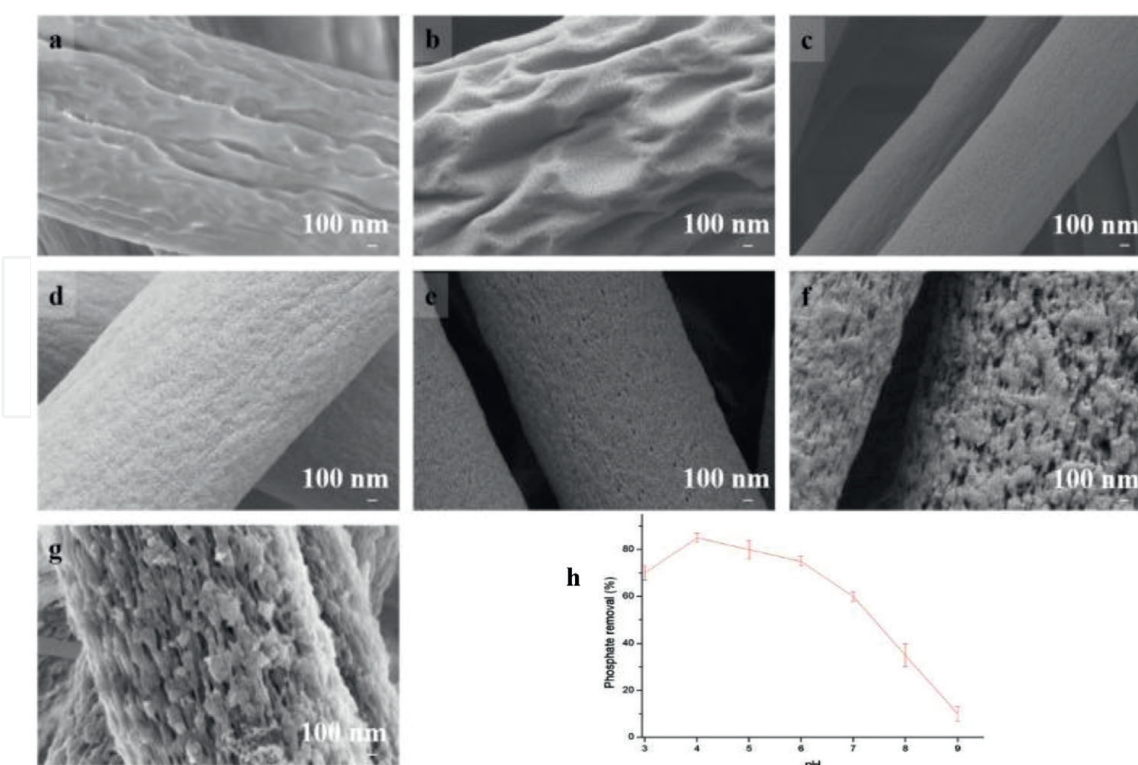


**Figure 5.** The FESEM micrographs of the fabricated electrospun nanofibrous membranes (a) PD0T10, (b) PD1T9, (c) PD3T7, (d) PD5T5, (e) PD7T3, (f) PD9T1, and (g) PD10T0 at 25 kV magnification, and phosphate adsorption (h) by fabricated electrospun PSF membrane [50].



to the formation of electrospun PSF nanofibers with a rough and porous surface (**Figure 5a-g**). Field emission scanning electron microscopy (FESEM), tensile strength technique, and contact angle measurements were applied for the investigation of the nanofibers obtained [50]. The results obtained did not correlate with the common conclusion that only a binary solvent provided formation of electrospun nanofibers with a rough or grooved surface [50]. The authors concluded that the dielectric constant was an important factor, besides boiling point and polymer solubility for binary solvent systems, which affected the phase separation in the solution and formation of nanofibers with non-smooth surfaces (**Figure 5h**).

Mazoochi et al. [3] studied the effect of processing parameters such as voltage applied and tip-to-collector distance (TCD) on the morphological features of electrospun PSF fibers. The formation of different morphologies, such as dry, bead-free, and continuous fibers, was observed without any breaking up to droplets. It was noted that jet flight time and electric field strength were directly affected by TCD. Decreasing TCD value decreased flight times and solvent evaporation time and increased electric field strength. This led to increasing bead generation. Rising in spinning distance provided the higher homogeneity of PSF fibers. The higher influence of the spinning distances was observed at higher applied voltages; the higher the applied voltage, the higher the surface charge of the jet and lower the beads formation.

## **5. Heat-resistant nanoporous thermosetting materials based on polycyanurates from cyanate ester resins**

Cyanate ether resins (CERs) are high-performance heat-resistant polymers that, unlike other polymers, have a highly regular polymer network structure. These polymers are also called polycyanurates (PCNs). They are obtained by polycyclotrimerization of dicyanate ethers of bisphenols. At present, many monomers of dicyanate ethers of bisphenols with different chemical structures have been synthesized [51–54]. CERs (PCNs) have attracted the attention of scientists and industrialists due to a unique set of physical and chemical properties: high thermal and thermooxidative stability (up to ~400–450°C), high glass transition temperatures (up to ~270–400°C), radiation resistance, chemical resistance to aggressive environments (alkalis, acids, alcohols, sea water, *etc.*) and adhesion to various metals (aluminum, titanium and their alloys, iron, *etc.*), carbon and glass plastics or fibers, as well as low dielectric losses ( $\epsilon \approx 2.64\text{--}3.11$ ), water absorption and absence of gas release during their synthesis, *etc.* [51–53]. As a result, CERs are currently used as structural and functional materials in microelectronics, aeronautics, and space structures as adhesives, binders, composite strips, nose radar domes, keels, heat shields, printed circuit boards, *etc.* [55].

Recently, a number of new methods of creating nanoporous film-forming materials based on thermostable PCNs have been developed [56]. Some of them were based on the modification of PCN networks by using a reactive porogen such as poly( $\epsilon$ -caprolactone) (PCL), which was first partially chemically incorporated into the PCN network, and then the nanoporous structures were formed by partial hydrolysis or extraction of unincorporated PCL chains. Another method for creating nanoporous structures used partial thermal degradation of PCN chains (at  $T \approx 250^\circ\text{C}$ ) with subsequent separation of destroyed chains. Four other suitable methods were developed to create a nanoporous structure in PCNs: (1) by using some high-boiling liquids (phthalates) as porogens; (2) by controlling the final degree of conversion of cyanate groups during the synthesis of PCN networks (with the subsequent selection of

unreacted chain fragments); (3) by using different ionic liquids as porogens during *in situ* synthesis of PCN networks followed by their removal during extraction; and 4) by irradiating PCN-based thin films with  $\alpha$ -particles to obtain track-etched membranes.

All the abovementioned nanomaterials based on PCNs are promising for use as high-tech thermally stable nanoporous membranes, demonstrating after complete extraction of the porogen a significant increase in He permeability and higher sorption abilities of  $\text{CO}_2$  and  $\text{O}_2$ , as well as approximately 1.5–1.8 times increased He/ $\text{O}_2$  and He/ $\text{CO}_2$  selectivity factors [57]. It was shown that before extraction of the porogen, both the mobility of the chains and the free volume determine the gas transport properties of nanoporous membranes based on PCNs. Whereas after extraction of the porogen, the volume content of pores and the pore size distribution become the predominant factors. Additional annealing of these nanomaterials in a rubber-like state (at  $T < T_g$ ) leads to an obvious modification of their nanoporous structure, which makes it possible to increase the separation capacity between large and small gas molecules in the glassy state (at  $T \geq T_g$ ) of the samples.

Nuclear technologies have also been used to create heat-resistant track-etched nanoporous membranes and filters based on PCNs. First, thermosetting grafted semi-IPNs based on PCN and linear polyurethane (LPU) were synthesized by stepwise *in situ* thermal curing, then the PCN/LPU thin films were irradiated with  $\alpha$ -particles followed by chemical etching of the created tracks [58]. SEM studies confirmed the formation of well-defined highly regular nanoporous structures in the films. FTIR spectroscopy measurements showed no significant changes in the chemical structure of the polymer components of the samples after the  $\alpha$ -irradiation and chemical etching procedures. The nanoporous PCN/LPU-grafted semi-IPNs had a narrow pore diameter distribution with an average pore diameter of about 12 nm. Differential scanning calorimetry (DSC) and thermogravimetric analysis (TGA) measurements showed that the nanoporous PCN/LPU films exhibited high thermal performance:  $T_g \sim 167^\circ\text{C}$  to  $\sim 199^\circ\text{C}$ ,  $T_{d5\%} \sim 293\text{--}359^\circ\text{C}$  and  $T_{d\text{max}} \sim 429\text{--}457^\circ\text{C}$ . The thermosetting nanoporous PCN/LPU track membranes also demonstrated effective gas transport properties with various gases such as  $\text{O}_2$ ,  $\text{CO}_2$ ,  $\text{N}_2$ , and  $\text{CH}_4$  (**Figure 6**). It was also found that the use of an additional  $\gamma$ -ray sensitization step and an increase in the chemical etching time improved the nanoporous structure and other properties of the

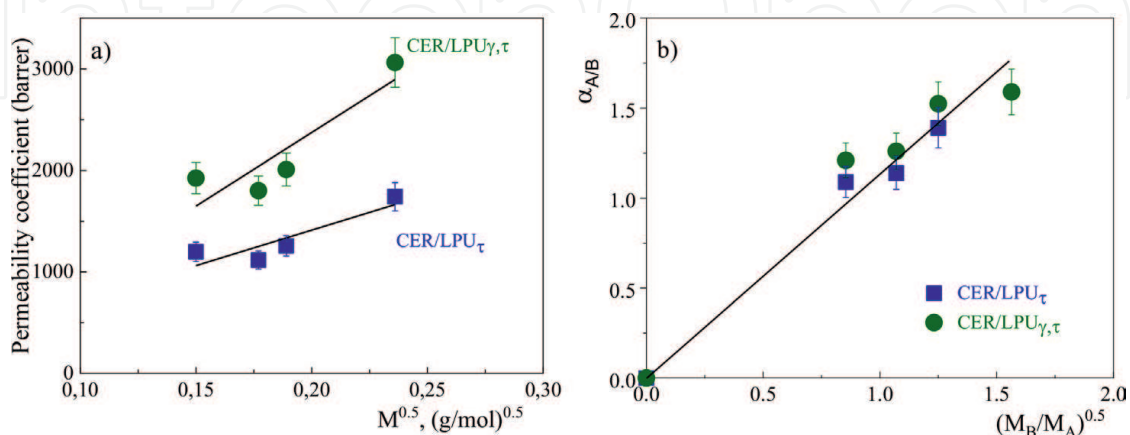


**Figure 6.**

Transport properties of different gases for nanoporous CER-based hybrid networks treated in different conditions: (a) permeability coefficients as a function of the inverse of the square root of the molar mass of the diffusing molecule; (b) gas selectivity values as a function of the ratio of the molecular weights of the diffusing molecules for the gas pairs  $\text{CO}_2/\text{O}_2$ ,  $\text{CH}_4/\text{N}_2$ ,  $\text{N}_2/\text{O}_2$ ,  $\text{CH}_4/\text{CO}_2$  [58].

developed nanoporous track membranes. Such materials open the way to numerous applications, for example, as ultrafiltration thermo- and chemically stable membranes for advanced technologies that can operate even under extreme conditions, that is, in aggressive environments, at high (> 250–400°C) or very low (up to –250°C) temperatures in a vacuum, under high radiation in space, *etc.*

## 6. Polysulfone/polycyanurate-based electrospun nanofibers with semi-IPN structure

Recently, we have implemented the electrospinning technique for preparing thermostable nanofibers with a structure of polysulfone/polycyanurate, polysulfone/polycyanurate/polybenzoxazine or polysulfone/poly(cyanurate-co-benzoxazine) semi-IPNs, and their structure-property relationships have been studied [59, 60]. The chemical structures of the components used for these studies are shown in **Figure 7**.

In this work, the nanofibers with a structure of polysulfone/polycyanurate semi-IPNs were prepared by electrospinning a mixed solution of PSF and dicyanate ester of bisphenol E (DCBE) (PSF/DCBE ratio was varied from 75/25 to 95/5) or 1–10 wt.% of the oligomer of dicyanate ester of bisphenol A (DCBA) (with cyanate groups conversion of about 25%) in DMF. The concentration of the polymer solution was equal to 21%. The electrospun nanofibers were fabricated using standard electrospinning equipment with a feeding rate of 8 mL/h, an accelerating voltage of 20 kV, and a distance between the needle tip and collector of 15 cm. The obtained nanofibers were dried at 25°C for 1.5 hours in a vacuum.

**Figure 8** shows the typical SEM micrograph for PSF/DCBA = 95/5 wt.%, PSF/DCBA = 90/10 wt.%, and PSF/DCBE = 75/25 wt.% electrospun nanofibers and the corresponding fiber diameter distributions. Electrospinning of PSF/DCBA = 95/5 wt.% and PSF/DCBA = 90/10 wt.% solutions resulted in very similar morphology with fiber diameter distributions of 350–1800 and 360–1600 nm, respectively (**Figure 8a,b**). The nanofibers were not entirely uniform, as they contained some oval-shaped structures, and some single fibers displayed diameters larger than 2 microns. With the increase in cyanate monomer DCBE (up to 25%) in the spinning dope, the nanofibers become thinner in diameters with narrower size distributions (**Figure 8c**). This was due to the substantial decrease in the viscosity of the spinning

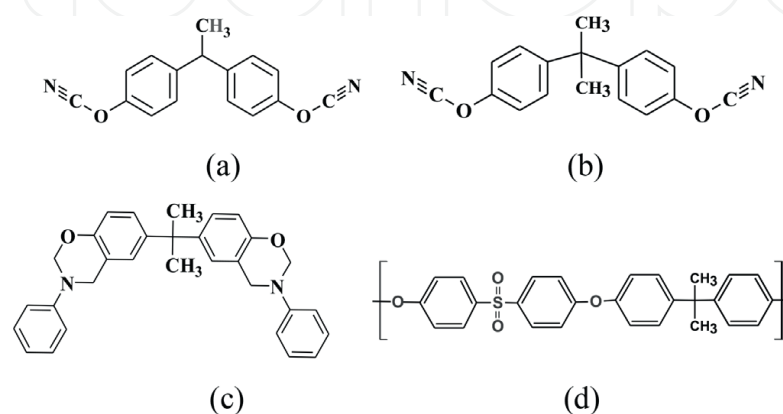


**Figure 7.** Chemical structure of (a) dicyanate ester of bisphenol E (DCBE), (b) dicyanate ester of bisphenol A (DCBA), (c) bisphenol-A based benzoxazine (BA-a), and (d) polysulfone (PSF,  $M_w = 35,000 \text{ g}\cdot\text{mol}^{-1}$ ).

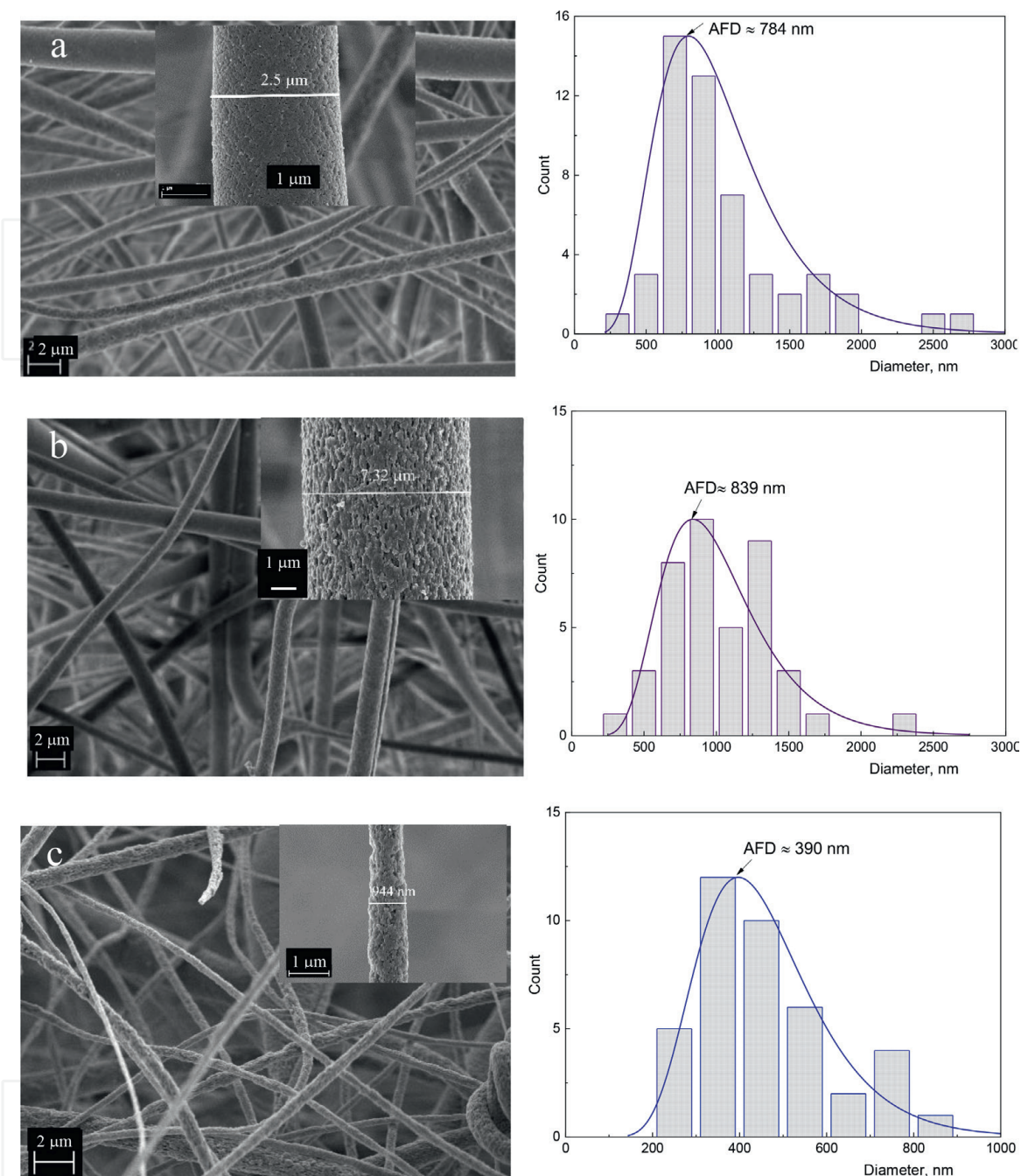


**Figure 8.** Typical SEM micrograph for electrospun nanofibers of different compositions (wt.%): (a) PSF/DCBA = 95/5, (b) PSF/DCBA = 90/10, and (c) PSF/DCBE = 75/25. The corresponding fiber diameter distributions are displayed on the right side.

solution with the increase in the content of the low-molecular DCBE monomer. It could also be seen that all the electrospun nanofibers showed high internal porosity.

The electrospun nanofibers with a structure of polysulfone/polycyanurate/polybenzoxazine semi-IPN were prepared by electrospinning from a mixed solution of PSF and PCN-BA prepolymer in DMF. The prepolymer poly(cyanurate-co-benzoxazine) (PCN/BA) was synthesized as follows: BA-a in the amount of 25 wt.% was added to liquid dicyanate ester of bisphenol E (DCBE) at 100°C, then the blend was heated to 120°C and vigorously stirred during 60 minutes. The prepolymer synthesized was a viscous liquid at room temperature. According to the calculations from the FTIR data, the conversion of cyanate groups of DCBE in the PCN/BA prepolymer

obtained was estimated as  $\alpha \approx 30\%$ . Electrospinning operational parameters such as applied voltage, working distance between the spinneret and the planar collector, flow rate, and temperature were 20 kV, 150 mm, 2.5 ml/h, and 20°C, respectively. The collected mat was placed under vacuum at 30°C to remove residual solvent.

To produce polysulfone/polycyanurate/polybenzoxazine semi-IPNs, the PSF/PCN-BA fiber meshes were cured using a step-by-step schedule: 1 hour at 80°C, 1 hour at 120°C, 1 hour at 150°C, 1 hour at 180°C, 1 hour at 220°C, and 1 hour at 250°C. After each heating step, the morphology of nanofibers was monitored using SEM, and the formation of triazine cycles of PCN and the oxazine ring opening of BA-a in PSF/PCN-BA were analyzed using FTIR.

Initially, four different polymer solutions were selected in an attempt to prepare PSF/PCN-BA nanofibers with two different PSF/PCN-BA ratios (60/40 and 70/30 wt.%) and two different concentrations (20% (wt/vol) and 30% (wt/vol)). **Figure 9** represents the typical SEM micrograph for nonwoven PSF/PCN-BA fiber mesh obtained. At lower concentrations (**Figure 9a,b**), the fibers were not completely uniform and contained some beads, twists, and ovoid structures. The fiber diameter of the electrospun fibers was varied from 110 to 270 nm for PSF/PCN-BA = 60/40 wt.% (20 wt/vol) and from 180 to 360 nm for PSF/PCN-BA = 70/30 wt.% (20 wt/vol) nanofibers. With the increase in concentration, the electrospun nanofibers became more uniform with larger diameters (ranging from 350 to 800 nm with some individual fibers measuring about 1.5 microns). At the same time, the PSF/PCN-BA = 60/40 wt.% (30 wt/vol) nanofibers exhibited some twists and were agglomerated and distorted at their cross-points (**Figure 9c**). **Figure 9d** shows that better-defined and more uniform nanofibers (fiber diameter distribution: 500–900 nm) were obtained from the PSF/PCN-BA = 70/30 wt.% (30 wt/vol) polymer solution.

To investigate the morphology of PSF/PCN-BA = 70/30 wt.% (30 wt/vol) electrospun nanofibers during the thermal curing of a cyanate/benzoxazine prepolymer and to control the formation of the cross-linked structure, respectively, SEM and IR spectroscopy studies were conducted. **Figure 10a** shows the FTIR spectra of individual DCBE, BA-a, and PSF. In the spectrum for neat DCBE, the characteristic bands at 2237 and 2266  $\text{cm}^{-1}$  denote  $\text{C} \equiv \text{N}$  stretching vibrations, and the characteristic absorption bands at 1500 and 1601  $\text{cm}^{-1}$  are due to the vibration of benzene ring. The FTIR spectrum of BA-a monomer includes the absorption bands at 1232 and 1159  $\text{cm}^{-1}$  assigned, respectively, to the antisymmetric stretching vibration of  $\text{C}-\text{O}-\text{C}$  and  $\text{C}-\text{N}-\text{C}$  of oxazine functionality. There is also the characteristic band at 947  $\text{cm}^{-1}$  which corresponds to the benzene ring mode that is attached to the oxazine ring. The spectrum of individual PSF contains bands with maxima at 1150 and 1324  $\text{cm}^{-1}$  corresponded to symmetric and asymmetric  $\text{S}=\text{O}$  stretching vibrations, band at 1244  $\text{cm}^{-1}$  assigned to  $\text{C}-\text{O}-\text{C}$  stretching vibrations, and bands at 874 and 833  $\text{cm}^{-1}$  are due to aromatic CH deformation vibration.

**Figure 10b** shows the evolution of FTIR spectra for PSF/PCN-BA electrospun nanofibers with thermal treatment. The absorption bands distinctive for all the individual components of unheated nanofibers are present in the spectrum. The intensities of the absorption bands with maxima at 2266–2235 and 947  $\text{cm}^{-1}$  start to decrease gradually with increasing the curing temperature from 120 to 150°C. After raising the curing temperature to 180°C, the aforementioned absorption bands disappear, demonstrating that cyanate and oxazine groups have been completely exhausted under the applied conditions. Typically, for the complete curing of the individual monomers DCBE and BA-a, temperatures of 177–200°C and  $\sim 200^\circ\text{C}$  are required,

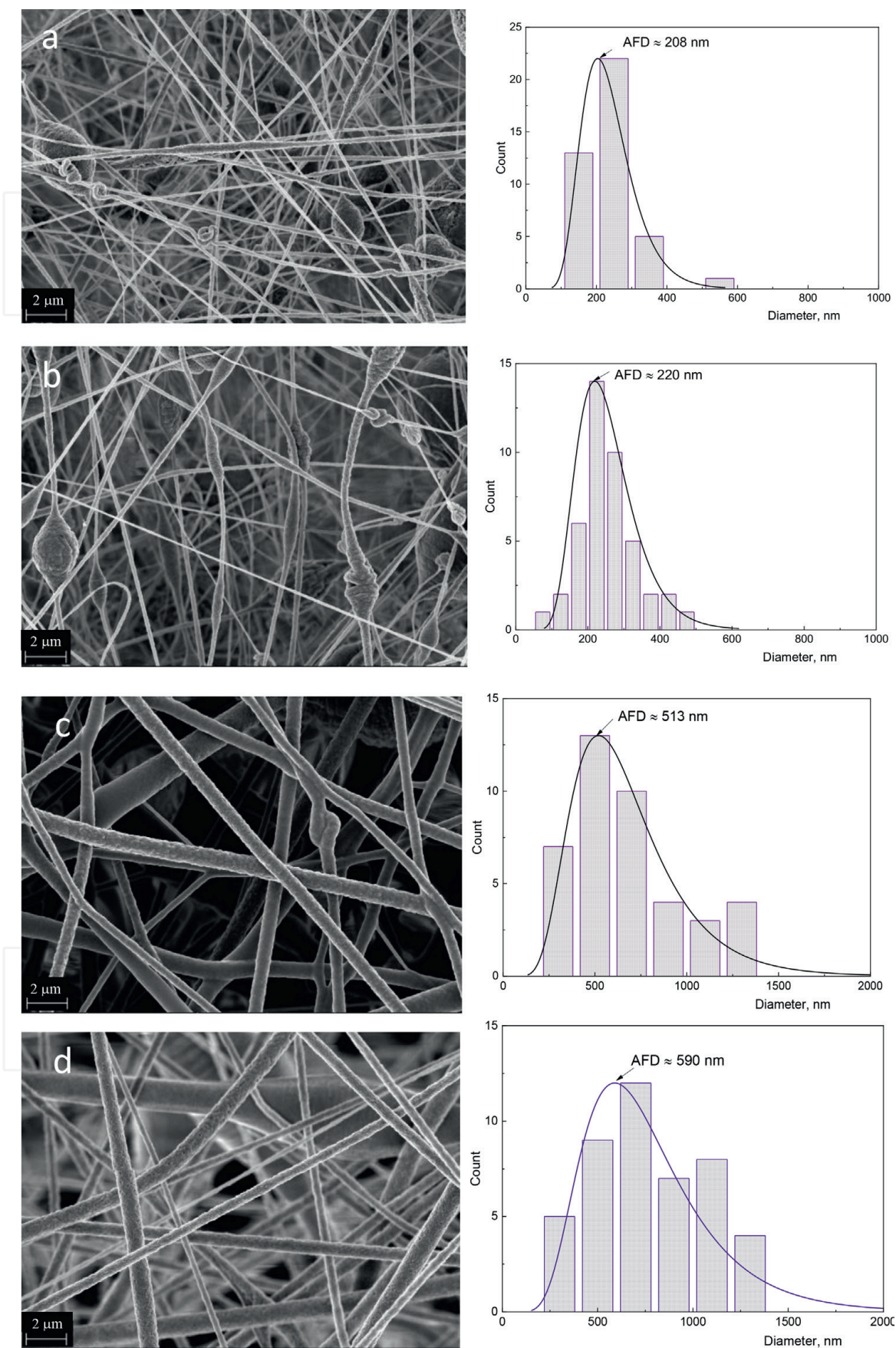


**Figure 9.** Typical SEM micrographs for the samples (wt.%): (a) PSF/PCN-BA = 60/40 (20 wt/vol), (b) PSF/PCN-BA = 70/30 (20 wt/vol), (c) PSF/PCN-BA = 60/40 (30 wt/vol), and (d) PSF/PCN-BA = 70/30 (30 wt/vol) electrospun nanofibers. The corresponding fiber diameter distributions are displayed on the right side.

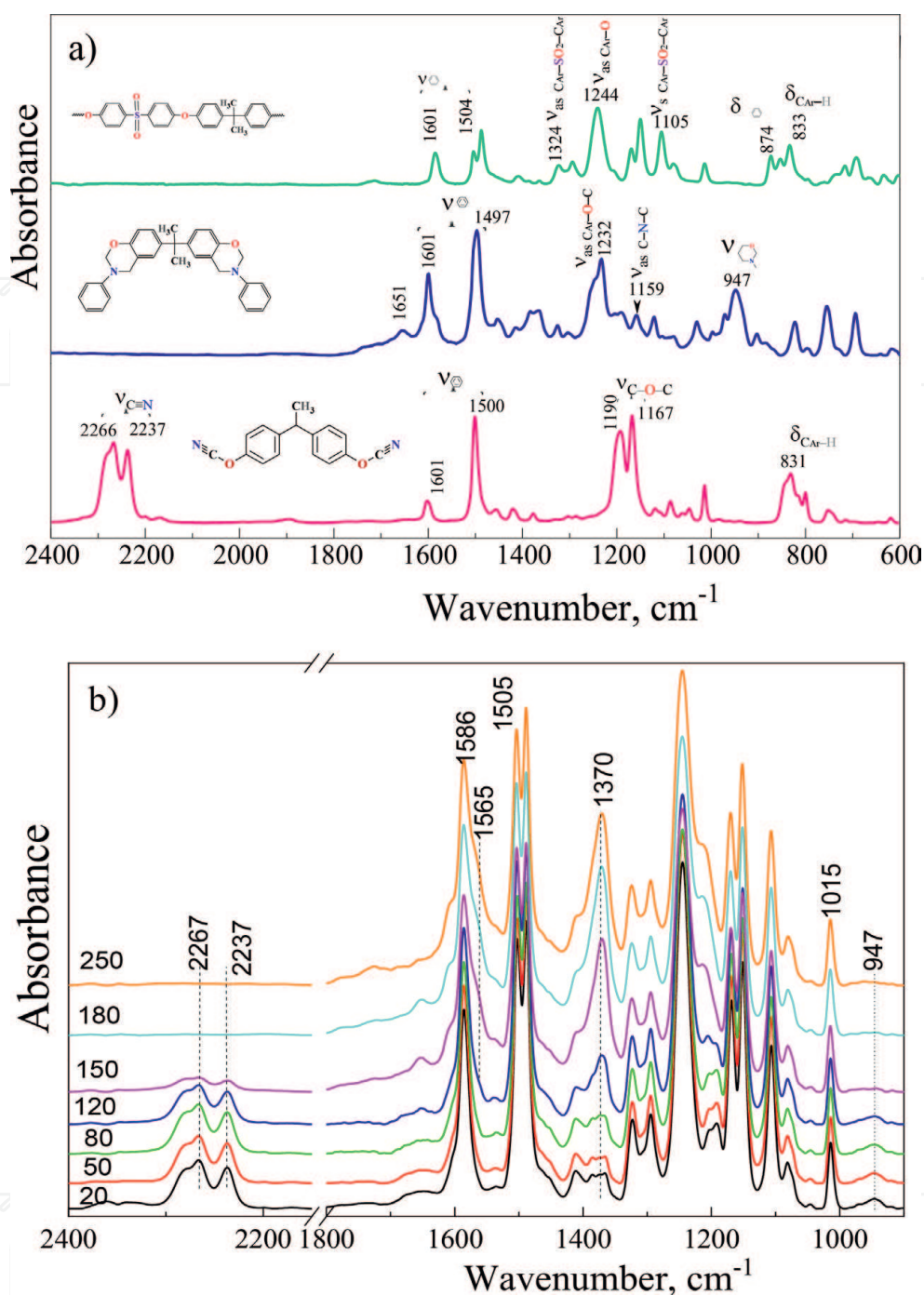


**Figure 10.** FTIR spectra of typical samples: (a) individual DCBE, BA-a, and PSF; (b) PSF/PCN-BA = 70/30 wt.% electrospun nanofibers cured at different temperatures (indicated in the spectra).

respectively [51–55]. Therefore, it can be concluded that in this ternary composition, the curing of DCBE and BA-a is completed at a lower temperature, probably due to a synergetic effect.

**Figure 11** shows the change in fiber morphology for PSF/PCN-BA = 70/30 (wt.%) electrospun fibers after their heat treatment during the synthesis of the PCN-BA component within the PSF fibers. It is obvious that the electrospun fibers retain their shape when heated to 80°C (**Figure 11a**). With a further increase in the synthesis temperature of PCN-BA as an IPN component to 120°C, a noticeable thickening of the fibers occurs (**Figure 11b**), apparently due to swelling of the PSF matrix of the

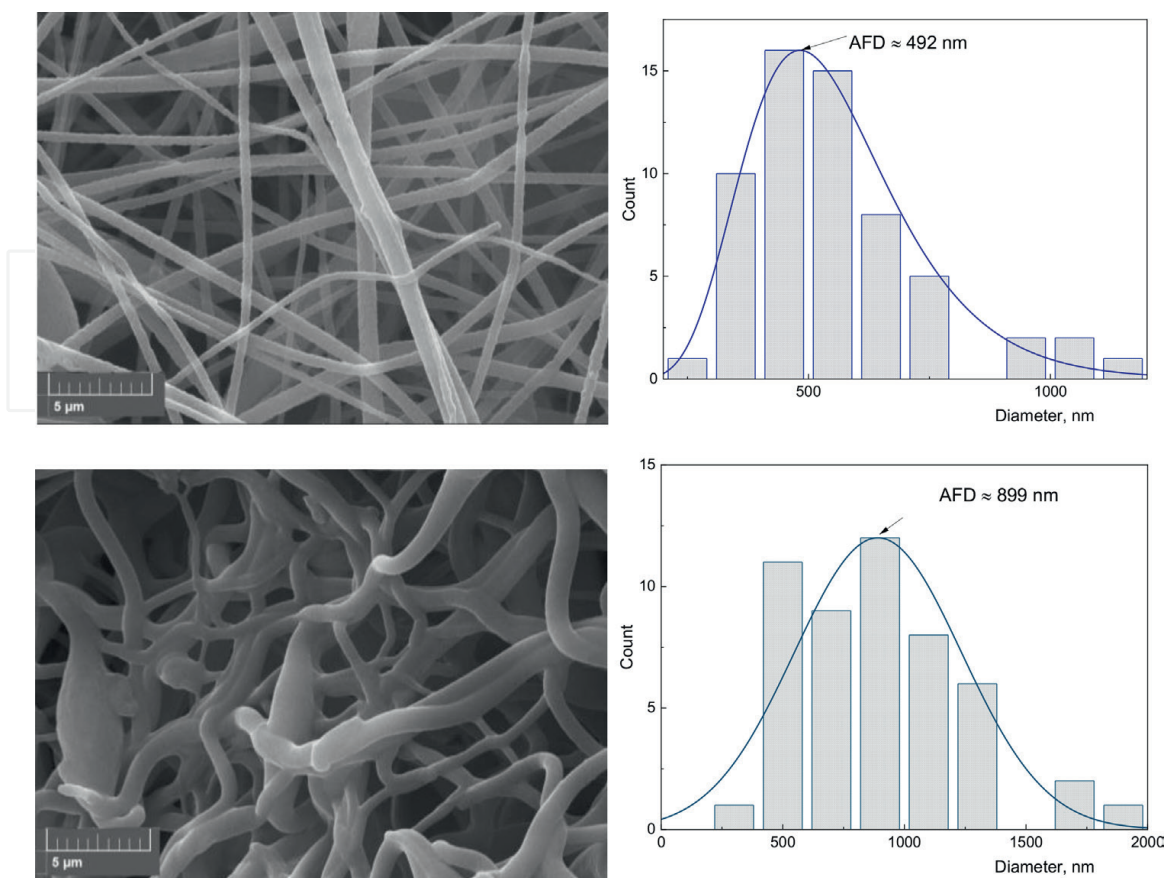


**Figure 11.** Typical SEM micrograph for PSF/PCN-BA = 70/30 (wt.%) electrospun nanofibers cured at different temperatures: (a) 80°C and (b) 120°C. The corresponding fiber diameter distributions are displayed in the right side.

electrospun fibers with the low-viscosity PCN-BA prepolymer. It can be concluded that the synthesis of the PCN-BA component of PSF/PCN-BA electrospun nanofibers should be carried out at temperatures below 80–100°C. Our new studies have shown that it is possible to significantly reduce the synthesis temperature (even up to room temperature) of polycyanurates or their copolymers by introducing various nanofillers, for example, amino-functionalized POSS.

The thermal stability of cured PSF/PCN-BA semi-IPNs was examined by TGA, and the thermogravimetric curve (TG) and corresponding derivative curve (DTG) are shown in **Figure 12**. For comparison, the TG and DTG curves for the hybrid PCN-BA thermoset obtained under the same curing conditions and for the pure PSF are presented in the plot. Two mass loss stages were observed in DTG curves for the PCN-BA hybrid thermoset and neat PSF. During the first stage of degradation (at a temperature of maximum degradation rate  $T_{d\ max1} \sim 421$  and  $535^\circ\text{C}$ , respectively for PCN/BA and PSF), thermal degradation of the polymers occurs, and during the second mass loss stages at  $T_{d\ max2} \sim 628$  and  $622^\circ\text{C}$ , respectively, the oxidation of decomposed residues derived from the first stage takes place. Cured PSF/PCN-BA film sample possess good heat resistance with the initial thermal-oxidative degradation temperature ( $T_{d5\%}$ ) above  $390^\circ\text{C}$ . The thermooxidative degradation in air of PSF/PCN-BA semi-IPN occurs in four stages: at  $T_{d\ max1} \sim 421^\circ\text{C}$ ,  $T_{d\ max2} \sim 542^\circ\text{C}$ ,  $T_{d\ max3} \sim 589^\circ\text{C}$ , and  $T_{d\ max4} \sim 658^\circ\text{C}$ . The mass loss of PSF/PCN-BA at the first low-intensity stage can be related to the thermal decomposition of the mixed PSF/PCN-BA microphase formed as a result of the interpenetrating of macromolecules of PCN-BA



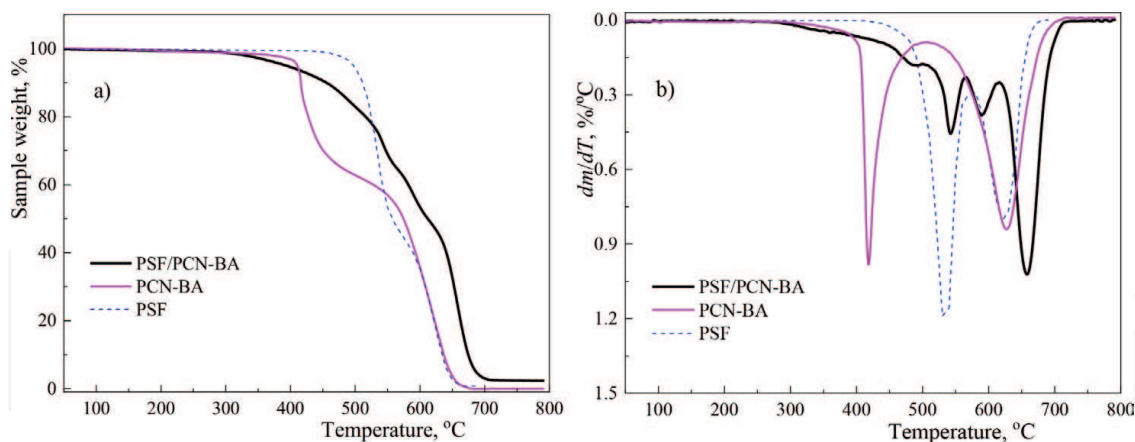


**Figure 12.**

TG (a) and DTG (b) curves for cured PSF/PCN-BA = 70/30 (wt.%) film sample with a structure of semi-IPNs, PCN-BA hybrid thermoset, and neat PSF (indicated in the plot).

and PSF during *in situ* synthesis. The mass loss at  $T_{d\ max2} \sim 542^\circ\text{C}$  can be attributed to the thermal decomposition of the PSF component. The mass losses with maxima rates at 589 and 658°C are caused essentially by oxidative processes in the composition. These results indicate that the PSF/PCN-BA semi-IPN has better thermal oxidative stability at temperatures higher than 600°C compared to their constitutive components.

The thermophysical properties of cured PSF/PCN-BA film sample with a structure of semi-IPNs compared to PCN-BA hybrid thermoset and neat PSF were studied by DSC (Figure 13).

Both PCN-BA and individual PSF have DSC traces typical for amorphous polymers with single glass transition temperatures,  $T_g$ , at  $\sim 196$  and  $\sim 184^\circ\text{C}$ , respectively. The DSC thermogram of the PSF/PCN-BA film sample shows one main endothermic transition corresponding to  $T_g \sim 185^\circ\text{C}$  of the PSF component in semi-IPNs. The presence of two other small endothermic transitions in the region of lower temperatures (at  $T \sim 130$ – $160^\circ\text{C}$ ) may indicate the formation of some microphase heterogeneity in the sample.

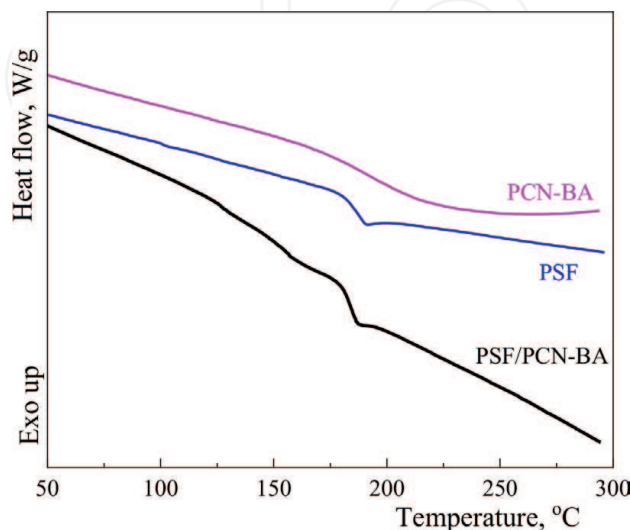


**Figure 13.**

DSC thermograms for PCN-BA hybrid thermoset and neat PSF, as well as for cured PSF/PCN-BA = 70/30 wt.% film sample with a structure of semi-IPNs (indicated in the plot).

Thus, our studies have shown the fundamental possibility of obtaining electrospun PSF/PCN-BA nanofibers with acceptable thermal properties. In addition, it is known that the polycyanurate component of these nanofibers, in addition to heat resistance, is characterized by high chemical resistance to various aggressive environments, as well as low dielectric losses and water absorption. Therefore, resulting electrospun fibers can potentially become useful components of various textile materials with an improved set of properties suitable for operation in aggressive environments over a wide temperature range.

## **7. Conclusions**

Over recent years, significant attention has been paid to the development of new directions toward the engineering of heat-resistant micro- and nanofibers based on thermosets and their nanocomposites, as well as thermoplastic/thermosetting polymers with a semi-IPN structure. Thus, this chapter addresses the main recent approaches and technical solutions for the creation of polymer micro or nanofibers by electrospinning. Miscellaneous systems have been investigated, including epoxy electrospun continuous micro- and nanofibers, submicron carbon nanotube–epoxy nanocomposite filaments, rigid fibers based on functional polynorbornenes with epoxy or carboxylic pendant groups, and core-shell nanofibers with a structure of semi-IPNs based on thermoplastic polyamide (PA) and thermosetting epoxy resin. The first experimental results for the creation of electrospun nanofibers with a semi-IPN structure based on polysulfone/polycyanurate (PSF/PCN) or polysulfone/polycyanurate-benzoxazine (PSF/PCN-BA) are discussed. The possibility of controlling the average diameter from ~220 nm up to ~900 nm for the PSF/PCN or PSF/PCN-BA based electrospun nanofibers is fixed by changing the composition as well as processing parameters. It was found that the synthesis of the PCN-BA component of PSF/PCN-BA electrospun nanofibers should be carried out at temperatures below 80–100°C, but our recent studies have shown the possibility to reduce the synthesis temperature (even up to room temperature) for PCN by using various nanofillers, for example, amino-functionalized POSS. Due to the unique properties of PCNs, that is, high heat- and chemical resistance to aggressive substances, low dielectric losses and low water absorption, PCN-containing electrospun fibers could potentially become useful as components in advanced materials with improved properties to work in aggressive environment over a range of temperatures.

## **Acknowledgements**

The work was supported by the National Academy of Sciences of Ukraine (NASU) and the “Center National de la Recherche Scientifique” (CNRS) through French-Ukrainian International Research Projects on Nanoporous Thermostable Polymer Materials “LIA POLYNANOPOR” and “IRP POLYTHERMAT”.

## **Conflict of interest**

The authors declare no conflict of interest.

IntechOpen

## Author details

Alexander Fainleib<sup>1\*</sup>, Olga Grigoryeva<sup>1</sup>, Olga Starostenko<sup>1</sup> and Daniel Grande<sup>2\*</sup>


1 Institute of Macromolecular Chemistry of the National Academy of Sciences of Ukraine, Kyiv, Ukraine

2 University of Strasbourg, CNRS, Institut Charles Sadron, Strasbourg, France

\*Address all correspondence to: [fainleib@i.ua](mailto:fainleib@i.ua) and [daniel.grande@ics-cnrs.unistra.fr](mailto:daniel.grande@ics-cnrs.unistra.fr)

## IntechOpen

---

© 2024 The Author(s). Licensee IntechOpen. This chapter is distributed under the terms of the Creative Commons Attribution License (<http://creativecommons.org/licenses/by/4.0>), which permits unrestricted use, distribution, and reproduction in any medium, provided the original work is properly cited. 

## References

- [1] Gopal R, Kaur S, Feng C, Chan C, Ramakrishna S, Tabe S, et al. Electrospun nanofibrous polysulfone membranes as pre-filters: Particulate removal. *Journal of Membrane Science*. 2007;**289**:210-219. DOI: 10.1016/j.memsci.2006.11.056
- [2] Xu Z, Gu Q, Hu H, Li F. A novel electrospun polysulfone fiber membrane: Application to advanced treatment of secondary bio-treatment sewage. *Environmental Technology*. 2008;**29**:13-21. DOI: 10.1080/09593330802008412
- [3] Mazoochi T, Hamadani M, Ahmadi M, Jabbari V. Investigation on the morphological characteristics of nanofibrous membrane as electrospun in the different processing parameters. *International Journal of Industrial Chemistry*. 2012;**3**:2. DOI: 10.1186/2228-5547-3-2
- [4] Jebamalar Leavline E, Asir Antony Gnana Singh D, Prasannanayagi S, Kiruthika R. A compendium of nano materials and their applications in smart nano textiles. *Research Journal of Nanoscience and Nanotechnology*. 2015;**5**:44-59. DOI: 10.3923/rjnn.2015.44.59
- [5] Xin JH, Daoud WA, Kong YY. A new approach to UV-blocking treatment for cotton fabrics. *Textile Research Journal*. 2004;**74**:97-100. DOI: 10.1177/0040517504074002
- [6] Yeo SY, Lee HJ, Jeong SH. Preparation of nanocomposite fibers for permanent antibacterial effect. *Journal of Materials Science*. 2003;**38**:2143-2147. DOI: 10.1023/A:1023767828656
- [7] Afifi AM, Nakano S, Yamane H, Kimura Y. Electrospinning of continuous aligning yarns with a 'funnel' target. *Macromolecular Materials and Engineering*. 2010;**295**:660-665. DOI: 10.1002/mame.200900406
- [8] Pillai CKS, Sharma CP. Electrospinning of chitin and chitosan nanofibres. *Trends in Biomaterial and Artificial Organs*. 2009;**22**:175-197
- [9] Fadil F, Nor Affandi ND, Misnon MI, Bonnia NN, Harun AM, Alam MK. Review on electrospun nanofiber-applied products. *Polymers*. 2021;**13**:2087. DOI: 10.3390/polym13132087
- [10] Choi J, Lee KM, Wycisk R, Pintauro PN, Mather PT. Sulfonated polysulfone/POSS nanofiber composite membranes for PEM fuel cells. *Journal of the Electrochemical Society*. 2010;**157**:B914-B919. DOI: 10.1149/1.3392294
- [11] Yoon KH, Kim KS, Wang XF, Fang DF, Hsiao BS, Chu B. High flux ultrafiltration membranes based on electrospun nanofibrous PAN scaffolds and chitosan coating. *Polymer*. 2006;**47**:2434-2441. DOI: 10.1016/j.polymer.2006.01.042
- [12] Wang H-S, Guo-Dong F, Li X-S. Functional polymeric nanofibers from electrospinning. *Recent Patents on Nanotechnology*. 2009;**3**:21-31. DOI: 10.2174/187221009787003285
- [13] Ma ZW, Masaya K, Ramakrishna S. Immobilization of Cibacron blue F3GA on electrospun polysulphone ultra-fine fiber surfaces towards developing an affinity membrane for albumin adsorption. *Journal of Membrane Science*. 2006;**282**:237-244. DOI: 10.1016/j.memsci.2006.05.027
- [14] Lannutti J, Reneker DH, Ma T, Tomasko D, Farson D. Electrospinning

for tissue engineering scaffolds. *Materials Science and Engineering: C*. 2007;**27**:504-509. DOI: 10.1016/j.msec.2006.05.019

[15] Schiffman JD, Elimelech M. Antibacterial activity of electrospun polymer mats with incorporated narrow diameter single-walled carbon nanotubes. *Applied Materials and Interfaces*. 2011;**3**:462-468. DOI: 10.1021/am101043y

[16] Min BM, Lee G, Kim SH, Nam YS, Lee TS, Park WH. Electrospinning of silk fibroin nanofibers and its effect on the adhesion and spreading of normal human keratinocytes and fibroblasts in vitro. *Biomaterials*. 2004;**25**:1289-1297. DOI: 10.1016/j.biomaterials.2003.08.045

[17] Lee SW, Choi SW, Jo SM, Chin BD, Kim DY, Lee KY. Electrochemical properties and cycle performance of electrospun poly(vinylidene fluoride)-based fibrous membrane electrolytes for Li-ion polymer battery. *Journal of Power Sources*. 2006;**163**:41-46. DOI: 10.1016/j.jpowsour.2005.11.102

[18] Hekmati AH, Rashidi A, Ghazisaeidi R, Drean JY. Effect of needle length, electrospinning distance, and solution concentration on morphological properties of polyamide-6 electrospun nanowebs. *Textile Research Journal*. 2013;**83**(4):1452-1466. DOI: 10.1177/0040517512471746

[19] Teo W, Ramakrishna S. A review on electrospinning design and nanofibre assemblies. *Nanotechnology*. 2006;**17**(14):R89-R106. DOI: 10.1088/0957-4484/17/14/R01

[20] Pakravan M, Heuzey MC, Ajji A. A fundamental study of chitosan/PEO electrospinning. *Polymer*. 2011;**52**(21):4813-4824. DOI: 10.1016/j.polymer.2011.08.034

[21] Islam MS, Ang BC, Andriyana A, Afifi AM. A review on fabrication of nanofibers via electrospinning and their applications. *SN Applied Sciences*. 2019;**1**:1248-1263. DOI: 10.1007/s42452-019-1288-4

[22] Isaac B, Taylor RM, Reifsnider K. Mechanical and dielectric properties of aligned electrospun fibers. *Fibers*. 2021;**9**(1):4. DOI: 10.3390/fib9010004

[23] Jaeger R, Schönherr H, Vancso G. Chain packing in electro-spun poly(ethylene oxide) visualized by atomic force microscopy. *Macromolecules*. 1996;**29**(23):7634-7636. DOI: 10.1021/ma9610673

[24] Taylor G. Disintegration of water drops in an electric field. *Proceedings of the Royal Society A*. 1964;**280**(1382):383-397. DOI: 10.1098/rspa.1964.0151

[25] Jalili R, Hosseini SA, Morshed M. The effects of operating parameters on the morphology of electrospun polyacrylonitrile nanofibres. *Iranian Polymer Journal*. 2005;**4**(12):1074-1081

[26] Li D, Xia Y. Electrospinning of nanofibers: Reinventing the wheel? *Advanced Materials*. 2004;**16**(14):1151-1170. DOI: 10.1002/adma.200400719

[27] Greiner A, Wendorff JH. Electrospinning: A fascinating method for the preparation of ultrathin fibers. *Angewandte Chemie International Edition*. 2007;**46**(30):5670-5703. DOI: doi.org/10.1002/anie.200604646

[28] Son WK, Youk JH, Park WH. Preparation of ultrafine oxidized cellulose mats via electrospinning. *Biomacromolecules*. 2004;**5**(1):197-201. DOI: 10.1021/bm034312g

[29] Shneider M, Zattelman R, Kaestner A, Greenfeld I, Wagner HD.

- Electrospinning of epoxy fibers: Effect of curing conditions on solution rheological behavior. *Journal of Applied Polymer Science*. 2023;**140**(38):e54437. DOI: 10.1002/app.54437
- [30] Aliahmad N, Biswas PK, Wable V, Hernandez I, Siegel A, Dalir H, et al. Electrospun thermosetting carbon nanotube–epoxy nanofibers. *ACS Applied Polymer Materials*. 2021;**3**:610-619. DOI: 10.1021/acsapm.0c00519
- [31] Commarieu B, Compaoré M, de Boëver R, Imbeault R, Leprince M, Martin B, et al. Ultra-high Tg thermoset fibers obtained by electrospinning of functional polynorbornenes. *Nanomaterials*. 2022;**12**:967-975. DOI: 10.3390/nano12060967
- [32] Nie X, WuS MA, Lu K, Wei Q. Carbon quantum dots embedded electrospun nanofibers for efficient antibacterial photodynamic inactivation. *Materials Science and Engineering: C*. 2020;**108**:110377-110387. DOI: 10.1016/j.msec.2019.110377
- [33] Chen B, Zhang Y, Mao C, Gan Y, Li B, Cai H. Research on electrospinning thermosetting-thermoplastic core-shell nanofiber for rapid self-healing of carbon fiber/epoxy composites. *Composites Science and Technology*. 2022;**227**:109577-109588. DOI: 10.1016/j.compscitech.2022.109577
- [34] Bartolotta A, Di Marco G, Lanza M, Carini G, D'Angelo G, Tripodo G, et al. Molecular mobility in semi-IPNs of linear polyurethane and heterocyclic polymer networks. *Journal of Adhesion*. 1997;**64**:269-286. DOI: 10.1080/00218469708010543
- [35] Rasouli M, Pirsalami S, Zebarjad SM. Optimizing the electrospinning conditions of polysulfone membranes for water microfiltration applications. *Polymer International*. 2019;**68**(9):1610-1617. DOI: 10.1002/pi.5858
- [36] Manawi Y, Kochkodan V, Atieh MA. Arabic gum as a novel pore-forming and hydrophilic agent in polysulfone membranes. *Journal of Membrane Science*. 2017;**529**:95-104. DOI: 10.1016/j.memsci.2017.02.002
- [37] Nechifor G, Voicu SI, Nechifor AC, Garea S. Nanostructured hybrid membrane polysulfone-carbon nanotubes for hemodialysis. *Desalination*. 2009;**241**:342-348. DOI: 10.1016/j.desal.2007.11.089
- [38] Xu Z, Liao J, Tang H, Li N. Antifouling polysulfone ultrafiltration membranes with pendent sulfonamide groups. *Journal of Membrane Science*. 2018;**548**:481-489. DOI: 10.1016/j.memsci.2017.11.064
- [39] Khalid A, Al-Juhani AA, Al-Hamouz OC, Laoui T, Khan Z, Atieh MA. Preparation and properties of nanocomposite polysulfone/multi-walled carbon nanotubes membranes for desalination. *Desalination*. 2015;**367**:134-144. DOI: 10.1016/j.desal.2015.04.001
- [40] Zheng Q, Wang P, Yang Y. Rheological and thermodynamic variation in polysulfone solution by PEG introduction and its effect on kinetics of membrane formation via phase-inversion process. *Journal of Membrane Science*. 2006;**279**:230-237. DOI: 10.1016/j.memsci.2005.12.009
- [41] Holda AK, Aernouts B, Saeys W, Vankelecom IFJ. Study of polymer concentration and evaporation time as phase inversion parameters for polysulfone-based SRNF membranes. *Journal of Membrane Science*. 2013;**442**:196-205. DOI: 10.1016/j.memsci.2013.04.017

- [42] Chakrabarty B, Ghoshal AK, Purkait MK. Ultrafiltration of stable oil-in-water emulsion by polysulfone membrane. *Journal of Membrane Science*. 2008;**325**:427-437. DOI: 10.1016/j.memsci.2008.08.007
- [43] Blanco JF, Sublet J, Nguyen QT, Schaetzel P. Formation and morphology studies of different polysulfones-based membranes made by wet phase inversion process. *Journal of Membrane Science*. 2006;**283**:27-37. DOI: 10.1016/j.memsci.2006.06.011
- [44] Ray SS, Chen S, Li C, Nguyen CN, Nguyen HT. A comprehensive review: Electrospinning technique for fabrication and surface modification of membranes for water treatment application. *RSC Advances*. 2016;**6**:85495-85514. DOI: 10.1039/C6RA14952A
- [45] Suja PS, Reshmi CR, Sagitha P, Sujith A. Electrospun nanofibrous membranes for water purification. *Polymer Reviews*. 2017;**57**:467-504. DOI: 10.1080/15583724.2017.1309664
- [46] Pirsalami S, Zebarjad SM, Daneshmanesh H. Evaluation and optimization of electrospun polyvinyl alcohol fibers via Taguchi methodology. *International Polymer Processing*. 2016;**31**:503-507. DOI: 10.3139/217.3278
- [47] Ma Z, Kotaki M, Ramakrishna S. Surface modified nonwoven polysulphone (PSU) fiber mesh by electrospinning: A novel affinity membrane. *Journal of Membrane Science*. 2006;**272**:179-187. DOI: 10.1016/j.memsci.2005.07.038
- [48] Feng C, Khulbe KC, Matsuura T, Tabe S, Ismail AF. Preparation and characterization of electrospun nanofiber membranes and their possible applications in water treatment. *Separation and Purification Technology*. 2013;**102**:118-135. DOI: 10.1016/j.seppur.2012.09.037
- [49] Wang R, Liu Y, Li B, Hsiao BS, Chu B. Electrospun nanofibrous membranes for high flux microfiltration. *Journal of Membrane Science*. 2012;**392-393**:167-174. DOI: 10.1016/j.memsci.2011.12.019
- [50] Chee TY, Yusoff ARM, Abdullah F, Mahmood WMAW, Jasni MJF, Malek NANN, et al. Fabrication, characterization and application of electrospun polysulfone membrane for phosphate ion removal in real samples. *Chemosphere*. 2022;**303**(3):135228-135235. DOI: 10.1016/j.chemosphere.2022.135228
- [51] Hamerton I, editor. *Chemistry and Technology of Cyanate Ester Resins*. London, UK: Chapman and Hall; 1994. p. 357p
- [52] Fainleib A, editor. *Thermostable Polycyanurates: Synthesis, Modification, Structure, and Properties*. New York, NY, USA: Nova Science Publisher; 2010. p. 362p
- [53] Ratna D. *Handbook of Thermoset Resins*. Shawbury, Shropshire, SY4 4NR, United Kingdom: iSmithers; 2009. pp. 132-153. ISBN: 978-1-84735-410-5
- [54] Kandelbauer A. Cyanate ester resins. Chapter 11. In: Dodiuk H, editor. *Handbook of Thermoset Plastics*. 4th ed. Oxford, UK: Elsevier Inc.; 2022. pp. 587-617. DOI: 10.1016/B978-0-12-821632-3.00004-X
- [55] VP MC. Resins for the hot zone, part II: BMIs, CEs, benzoxazines and phthalonitriles. *High-Performance Composites*. 2009;**21**:49-54. Available from: <https://www.compositesworld.com/articles/>

resins-for-the-hot-zone-part-ii-bmises-benzoxazinesand-phthalonitriles  
[Accessed: August 18, 2009]

[56] Fainleib AM, Grigoryeva O, Starostenko O, Gusakova K, Grande D. Thermostable Nanoporous Polycyanurates. Kyiv: Akadempriodyka; 2023. 112 p. DOI: 10.15407/akadempriodyka.477.112

[57] Gusakova K, Fainleib A, Espuche E, Grigoryeva O, Starostenko O, Gouanve F, et al. Nanoporous cyanate ester resins: Structure–gas transport property relationships. *Nanoscale Research Letters*. 2017;**12**:305(1-9). DOI: 10.1186/s11671-017-2071-3

[58] Grigoryeva O, Fainleib A, Starostenko O, Gusakova K, Sakhno V, Borzakovskiy A, et al. Thermally stable nanoporous cyanate ester resin/linear polyurethane networks created by nuclear technologies. *Polymer*. 2021;**228**:123831(1-11). DOI: 10.1016/j.polymer.2021.123831

[59] Fainleib A, Grigoryeva O, Starostenko O, Michely L, Nhuyen T-T-T, Grande D. Electrospun nanofibers based on *in situ* synthesized polycyanurate-polysulfone semi-IPNs. In: Proceedings of the X International Scientific-Technical Conference “Advance in Petroleum and Gas Industry and Petrochemistry” (APGIP-10); 18-23 May. Lviv, Ukraine: The Publishing House of Lviv Polytechnic; 2020; Lviv. p. 321

[60] Fainleib A, Grigoryeva O, Starostenko O, Michely L, Nhuyen T-T-T, Grande D. Thermal properties of polysulfone-polycyanurate electrospun nanofibers. In: Book of Abstracts of the 1st International Research and Practice Conference “Nanoobjects and Nanostructuring” (N&N-2020); 20-23 September. Lviv, Ukraine: Research and Publishing Center of the Shevchenko Scientific Society; 2020; Lviv. p. 118